Available online at www.sciencedirect.com
SCIENCE DIRECT
Coastal Engineering 53 (2006) 737–748
Coastal Engineering
An International Journal for Coastal, Harbour and Offshore Engineers
www.elsevier.com/locate/coastaleng

# A fuzzy–neural hybrid system of simulating typhoon waves

Hsien-Kuo Chang *, Wei-An Chien

*Department of Civil Engineering, National Chiao Tung University, 1001 Ta Hsuech Road, Hsinchu, 300, Taiwan*

Received 21 March 2005; received in revised form 22 September 2005; accepted 17 February 2006
Available online 19 April 2006

**Abstract**

This study addresses a fuzzy–neural hybrid system of simulating typhoon waves. A membership function based on the fuzzy theory is expressed by a union Gaussian function to illustrate the rapid wave decaying. Four areas separated by two lines which intersect at the Hua-Lien harbor indicate the case of typhoon's position and propagation. Better simulation performance of the peak wave heights and their occurrence time in both the learning stage and the verification stage simulated by the NF2 model than by the NF1 model is identified. The wave decaying due to land effect is well described by the NF2 model. The NF2 model is applicable for well simulating typhoon waves during the whole period of a typhoon approaching to Taiwan.


*Keywords:* Fuzzy–neural hybrid system; Land effect; Typhoon wave simulation

## 1. Introduction

Coastal erosion and marine hazard disaster often occur after a typhoon brings torrential rain and strong wind. Taiwan situated on the western Pacific Ocean suffers from 3.5 typhoons per year passing through or around Taiwan from averaging more than 100-year typhoon records. Therefore, several typhoon wave models have been used to calculate typhoon waves in Taiwan using the modified SWAN model (Hsu et al., 2005), Wave-Watch-III, MIKE-21. These models are generally developed to solve the energy balance equation in finite difference or finite element form through many grids over the water area where active generation is taking place. However, in this approach, the winds sometimes obtained by some wind models at all grids are required beforehand. Expert works in computer processing is also demanded. The computational time of a numerical model mainly depends on the number of grids that is generally enormous. Commonly these numerical models take long time to calculate typhoon waves of each typhoon at all grids in the entire domain. For practical engineering use, it is very necessary to provide fast wave calculation for a marine hazard alarm system, which can afford to fast update wave conditions around Taiwan when a typhoon is approaching to Taiwan, of ship navigation and disaster prevention.

Empirical prediction models for wave height and period have been proposed in simplified form, such as JONSWAP prediction graphs (Hasselmann et al., 1973), SMB prediction graphs (Bretschneider and Tamaye, 1976), Donelan method (Donelan, 1980; Donelan et al., 1985), and Krylov method (Koylov, 1966), or Shore protection manual (1984). The prediction formulas of wave height and period are presented in an explicit form for a fetch-limited condition or for a duration-limited condition. When the fetch length and wind speed and duration are obtained, the explicit expressions can fast determine the wave height and period at a point of interest. An examination on the SPM formulas against other methods carried out by Bishop et al. (1992) showed that the SPM method tends to overestimate wave height and period. Both Donelan's and Krylov's methods consider the difference between wind and wave directions. In most of these simplified empirical methods, wind and wave directions are assumed to be the same. Some supplements regarding to finite water depth are proposed to modify the basic properties of the empirical formulas. Hurdle and Stive (1989) proposed alternative formulas that asymptotically match the SPM expressions in deep water and shallow waters, for small and large fetch lengths. The literature review can refer to Massel (1996) and Goda (2003).

* Corresponding author.
*E-mail address:* hkc@faculty.nctu.edu.tw (H.-K. Chang).

0378-3839/$ - see front matter © 2006 Elsevier B.V. All rights reserved.
doi:10.1016/j.coastaleng.2006.02.003

The artificial neural network (NN) is an effective tool because of its high functioning with fast computation to solve the problems of high nonlinearity and of multi-variables. An NN model can be developed to establish suitable mathematical mapping between input and output variables by self-learning and self-adaptation. Thus NN has widely been implemented in different areas. Current works of using neural network for wave prediction and metrological science have been carried out by Deo and Shidhar Naidu (1998), Deo and Kiran Kumar (2000), Deo et al. (2001, 2002), Deo and Jagdale (2003), Makarynskyy (2004), Balas et al. (2004) and Agrawal and Deo (2002).

Typhoon waves induced by strong winds inside a typhoon in some days differ from monsoon waves acted by long-term monsoon. The authors particularly developed two NN typhoon wave models for the eastern water of Taiwan. In model development the physical relation between empirical formulas of wave prediction is considered to choose some suitable input variables in the input layer of an NN. This basic NN model can fairly calculate the peak wave height and its occurrence time of each typhoon.

However, the obtained typhoon wave data are not many so that the basic NN model cannot be well trained to fit all possible typhoon's paths and scales. To overcome the limitation of collected data Chang and Chien (2006) applied multi-trend functions instead of traditional transfer functions in a neural network to functionally fit the relationship between the inputs and the output and established the NN–MT model. The NN–MT model provides more stable and accurate calculation on wave heights before a typhoon reaches Taiwan.

Taiwan is an island of 385 km long in north–south and 143 km wide in east–west. About two-thirds of the island is covered with lush forested mountains. Jade Mountain at 3952 m above sea level is the tallest peak in Taiwan. Indeed some high mountains in Taiwan play an important role in changing the wind distribution of a typhoon around Taiwan and weakening the wind speed. The weakened winds result in a corresponding wave's decay. The interaction between typhoon winds and land is so complex that so far the existing parametric wind models are hard to accurately calculate the wind speeds inside a typhoon mount over the land. An efficient land modification on wind speeds is still unavailable.

The problem of land effect on winds can be solved by an NN model with a good construction that is established by using proper input variables and sufficient data to determine valid weight and bias matrices of an NN. The construction of an NN depends on the complexity of a problem and the number of input parameters. Commonly more neurons in each layer of an NN are required to connect possible relations between input and output variables for a complicated problem than those for a simple problem. However, due to the increase of neurons in each layer of an NN, sufficient data and much computational time are necessary to decide the suitable weight and bias matrices of the NN. When training data are less or ill-distributed the trained NN model possibly gives worse simulation. The present problem of land effect on winds is complicated and the number of collected wave data is not many enough. Thus the previous NN models can be applicable for accurately predicting the peak wave heights and their occurrence times, but fail to calculate the decaying wave heights when a typhoon approaches to Taiwan.

A fuzzy inference system (FIS) providing vague conjecture in terms of IF–THEN rules is commonly used to predict uncertain systems. FIS do not require knowledge of underlying physical process as a precondition. Thus it has been applied to different subjects, such as reservoir operation (Russel and Camplell, 1996; Shrestha et al., 1996; Dubrovin et al., 2002; Ponnambalam et al., 2003), rainfall forecasting (Yu et al., 2005) and metrological studies (Bardossy et al., 1995; Galambosi et al., 1998; Hiraoka et al., 1999). If the subject is complex and training data is less, a common adaptive-Network-Based FIS (ANFIS) with many IF–THEN rules, which is a combination of ANN and FIS, can not afford to serve good simulation.

In order to solve the complicated problem of the land effect on winds, this paper employs a neural network and FIS together to set up a fuzzy–neural hybrid wave model for accurately simulating wave heights when the obtained wave data is not sufficient. The previous NN–MT model is used to simulate wave heights first and then some specified membership functions which describe the land effect on winds in a typhoon are used to correct pre-estimated wave height. The proposed fuzzy–neural hybrid wave model with specified parameters in the membership function of FIS differs from ANFIS.

## 2. A brief introduction to the previous NN models

### 2.1. The original BPNN wave model

Through empirical formulae of wave prediction and energy action balance equation, the key parameters of a typhoon's waves at a point of interest are found to express a function of the significant wave heights

$$H_s = F_1(V_{10},\ V_f,\ r,\theta_1,\ \theta_2) \tag{1}$$

where $V_{10}$ is local wind speed at 10 m above mean sea level; $V_f$ is the moving speed of a typhoon; $(r,\theta_1)$ is the distance and azimuth between the point of interest and the center of the typhoon and $\theta_2$ is the angle of an interesting point in a typhoon between the typhoon moving direction and the radial direction from the typhoon's eye to that point. The sketch definition of $r,\theta_1$ and $\theta_2$ is depicted in Fig. 1.

When a typhoon moves, accelerates or changes direction, the preceding and subsequent winds affect local waves. A sequence of positions of a moving typhoon offers information that yields the speed of the typhoon at any position. The speed $V_f$ can be omitted from Eq. (1) if the earlier and subsequent positions of a typhoon are available. The sequential input of $V_{10}$, $r,\theta_1$ and $\theta_2$ is considered by another NN model. Significant wave heights can therefore be expressed as a set of preceding and subsequent positions of local winds and the center of the typhoon, as follows.

$$H_s(t) = \sum_{m=0}^{n} a_m F_2(V_{10},\ r,\theta_1,\ \theta_2;\ t - m\Delta t) \tag{2}$$

where $\Delta t$ is the sampling rate and $a_m$ is the coefficient.

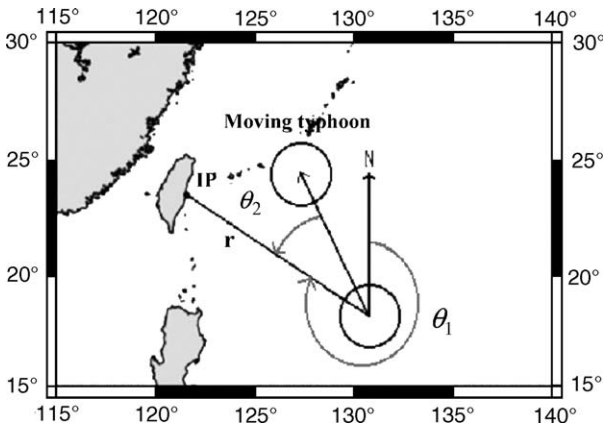


Fig. 1. Sketch definition of the coordinates $(r,\theta_1)$ and the angle $\theta_2$.

Based on Eqs. (1) and (2), Back-Propagation Neural Network (BPNN) is selected by Chang et al. (2003) to implement the typhoon wave model. The common Satlin function in the MATLAB software (Demuth and Beale, 2001) is used for the transfer function. If the relationships between the input and output are uncertain and complex, then the number of neurons in the first hidden layer can be increased to determine their relationships. Lippman (1987) addressed that a 2-hidden-layer NN is sufficient to simulate a problem that includes a highly nonlinear interaction or discontinuity. According to Mirchandani and Cao's (1989) formula of hidden nodes in neural nets, 80 neurons were suggested in the first hidden layer of the NN model. The second hidden layer contains 40 neurons to integrate the weightings in the first hidden layer and to connect weightings in the second layer to the output, $H_s$.

### 2.2. The NN–MT model

On account of wind distribution in a typhoon and data regression some trend transfer functions are introduced by Chang and Chien (2006) to describe the relationship between the input variables, which are $V_{10}$, $r$,$\theta_1$, and $\theta_2$, and wave height. The construction of the original NN–MT model of Chang and Chien (2006) is shown in Fig. 2. The input parameters and their corresponding multi-trend transfer functions of the NN–MT model are list in Table 1. The NN–MT model mainly attempts to enhance the functional relationships between the normalized input data and the normalized wave heights by using seven kinds of trend transfer functions to determine normalized data,

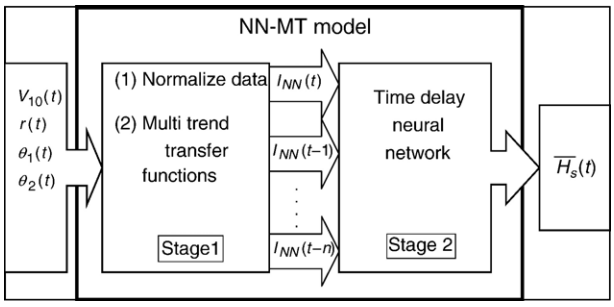


Fig. 2. The construction of the previous NN–MT model.

Table 1
The normalized input parameter and their corresponding multi trend transfer functions used in the NN–MT model of Chang and Chien (2006)

| Normalized inputs | Multi trend transfer functions |
|---|---|
| Wind speed, $\overline{V}_{10}$ | $f_{\overline{V}10} = \dfrac{2}{\left(1+e^{(-2\times\overline{V}_{10})}\right)} - 1$ |
| Radial distance, $\overline{r}$ | $f_{\overline{r}} = \mathrm{Max}\left(f_{r_1}, 0.5f_{r_2}, 0.3f_{r_3}, 0.2f_{r_4}\right)$ where $f_{\overline{r}_1} = e^{\frac{1(\overline{r}-c)^2}{2\sigma^2}}$, $i$=1,2,3,4 and coefficients $(c, \sigma)$ for each port are (0, 0.05) for $f_{r_1}$; (0.15, 0.1) for $f_{r_2}$;(0.2, 0.3) for $f_{r_3}$;(0.4,0.5) for $f_{r_4}$ |
| Azimuth, $\overline{\theta}_1$ | $f_{\overline{\theta}_1} = \overline{\theta}_1, \quad 0 \le \overline{\theta}_1 \le 1$ |
| Movement angle, $\overline{\theta}_2$ | $f_{\theta_2} = \mathrm{Max}\left(e^{\frac{-(\overline{\theta}_2-c_1)^2}{2\sigma_1^2}}, e^{\frac{-(\overline{\theta}_2-c_2)^2}{2\sigma_2^2}}\right) f_{\overline{r}}, \quad c_1 > c_2$ <br> $= f_{\overline{r}}, \quad c_1 < c_2$ <br> where coefficients $(c_1, \sigma_1, c_2, \sigma_2)$in each port are (0.66, 0.05, 0.84, 0.05) for $f_{\overline{\theta}_{21}}$; (0.41, 0.05, 0.59, 0.05) for $f_{\overline{\theta}_{22}}$; (0.16, 0.05, 0.34, 0.05) for $f_{\overline{\theta}_{23}}$ and (0.91, 0.05, 1.0, 0.05) or (0.0, 0.05, 0.09, 0.05) for $f_{\overline{\theta}_{24}}$ |

$f_{\overline{V}_{10}}, f_{\overline{r}}, f_{\overline{\theta}_1}, f_{\overline{\theta}_{21}}, f_{\overline{\theta}_{22}}, f_{\overline{\theta}_{23}}$, and $f_{\overline{\theta}_{24}}$. $\theta_2$ indicates the wind speed distribution in radial direction. It is common sense that the wind speed is stronger in the right-hand semicircle than that in the left-hand semicircle. Thus $\theta_2$ is an important factor affecting wave height. It is hard to hold a well-learned NN model from several wind data without almost uniform distribution by $\theta_2$. Thus the authors separate the wind speed distribution of Holland wind model by $\theta_2$ into four quarters, shown in Fig. 3. The trend functions $f_{\overline{\theta}_{21}}, f_{\overline{\theta}_{22}}, f_{\overline{\theta}_{23}}$, and $f_{\overline{\theta}_{24}}$ with different bell-shaped function show different effect of an approaching typhoon on waves of a point of interest. The suggested trend transfer function for $\theta_2$ resulted from the Holland wind model that fits open sea.

Cumulative waves with sequentially different speeds propagating from a far distance possibly together reach the point of interest at time $t$. Thus the wave height observed at the time $t$ maybe result from a sequence of wind at time $t-n\Delta t$ where $\Delta t$=1 h is the time interval of wave data acquisition and

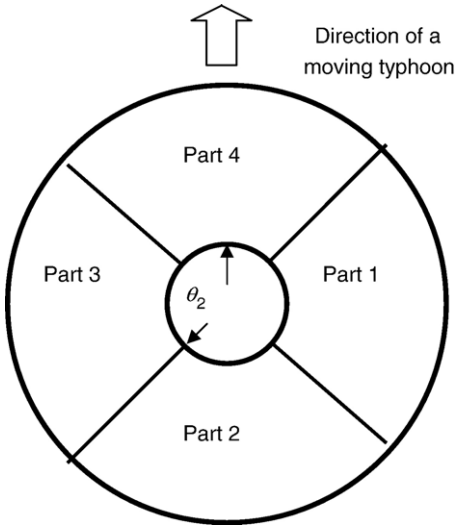


Fig. 3. Schematic diagram of four quarters of the wind speed distribution in a typhoon.

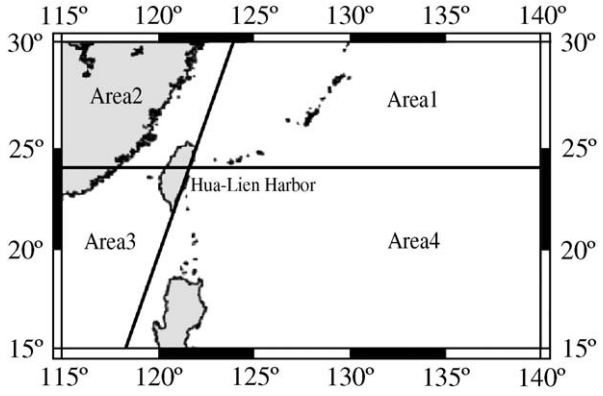


Fig. 4. Definition sketch of four areas separated for showing land effects on typhoon waves at the Hua-Lien harbor.

$n=1, 2, \ldots, 24$ is the delay time. Wind effect of 24-h time delay on the significant wave heights in the NN–MT model is also considered. The BPN network in the present NN–MT model is expressed as

$$H_{\mathrm{sMT}} = \sum_{n=0}^{24} a_n \cdot f[\mathbf{W} \cdot [\mathbf{I}]_{\mathrm{MT}} + \mathbf{b};\ t-n] \tag{3}$$

where $f$ represents the transfer function; $a_n$ is the weights of which the values are evaluated by the optimal procedure in the BPN network; $\mathbf{I}_{\mathrm{MT}} = [f_{\bar{V}_{10}}, f_{\bar{r}}, f_{\bar{\theta}_1}, f_{\bar{\theta}_{21}}, f_{\bar{\theta}_{22}}, f_{\bar{\theta}_{23}}, f_{\bar{\theta}_{24}}]^T$ is the input vector; **W** and **b** are the weight matrix and the bias matrix, and $n$ is the time lag.

## 3. Development of the fuzzy–neural hybrid wave model

### 3.1. Membership function for land effect

The range of land effect on typhoon waves can be surrounded from discriminating the time of wave's decaying and corresponding positions of the typhoon. From the data of decaying waves and corresponding typhoon's positions and scales wave attenuation depends on the land roughness and space, the membership function of a fuzzy inference system can describe the fuzzy relation between waves and wind speed of a typhoon that is changed by land effect.

The membership function related to land effect and wind-speed distribution in a typhoon is established for the Hua-Lien harbor in this paper. The Hua-Lien harbor is located at the center of eastern coast in Taiwan shown in Fig. 4. The whole island of Taiwan places on the western side of the Hua-Lien harbor. The wind-speed distribution of a typhoon in the right semicircle differs from that in the left semicircle due to the differently consultant velocity from the gradient wind velocity and the movement velocity of the typhoon. In order to indicate the land effect and different wind-speed distribution in a typhoon, two lines interacting at the Hua-Lien harbor separate the whole regions into four areas which are denoted by Area 1–Area 4 and shown in Fig. 4. The four separated areas are to indicate whether a typhoon is affected by the land and the Hua-Lien harbor is located either in the right semicircle or in the left semicircle of the typhoon. Both Area 1 and Area 4 demonstrate that the position of a typhoon is in the eastern side of the Hua-Lien harbor. When a typhoon located in Area 1 is approaching to the Hua-Lien harbor, the Hua-Lien harbor is located in the left semicircle. When a typhoon is located in Area 4, the Hua-Lien harbor is located in the right semicircle. Area 2 and Area 3 show the location of the Hua-Lien harbor being in either the left semicircle or the right one.

Fig. 5 shows wave heights at the Hua-Lien harbor at the corresponding positions $(r,\theta_1)$ for all typhoons collected. When a typhoon is located in Area 2 and Area 3 and near the Taiwan ($30° < \theta_1 < 210°$, $r < 500$), the waves display faster decaying than those when a typhoon is located in Area 1 and Area 4 and near the Taiwan ($210° < \theta_1 < 360°$, $r < 500$). When a typhoon is far

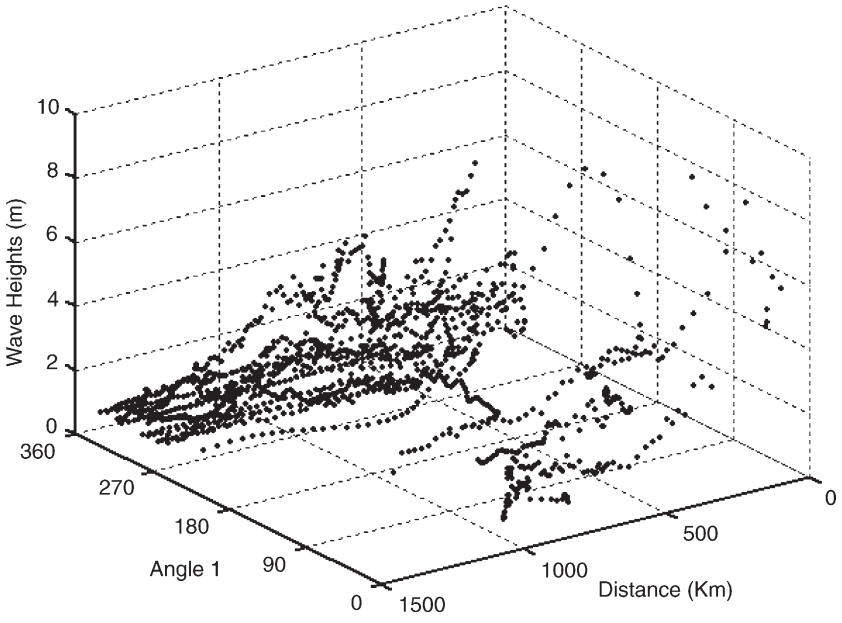


Fig. 5. Wave heights observed at the Hua-Lien harbor for all typhoons collected.

from Taiwan by a distance of more than 500 km, the waves decay more slowly than those when a typhoon is near Taiwan. The performance of wave variations can be described by a union Gaussian function which forms a membership function used in a fuzzy system.

A membership function includes three components. The first component of the membership function is to deal with the wind variations in the Area 1 and Area 4 in which a typhoon is located at the eastern open sea and its outer region senses the land. The maximum radial storm range at rank 7 of a typhoon, of which the wind speed is at a range of 13.9–17.1 m/s in Beaufort wind table, is about 500 km. This component can be defined as $MF_1$ and expressed by Eq. (4) in terms of two independent variables, $r$ and $\theta_1$. The value of $MF_1$ decreases from 1 to 0.2 as $r$ decreases from 500 km to 0 km.

$$\begin{aligned} MF_1(r,\theta_1) = {} & \mathrm{Max}\left(e^{\frac{-(r-c_1)^2}{2\sigma_1^2}}, e^{\frac{-(r-c_2)^2}{2\sigma_2^2}}\right) \\ & \times \mathrm{Max}\left(e^{\frac{-(\theta_1-c_3)^2}{2\sigma_3^2}}, e^{\frac{-(\theta_1-c_4)^2}{2\sigma_4^2}}\right) \\ & + \mathrm{Max}\left(e^{\frac{-(r-c_5)^2}{2\sigma_5^2}}, e^{\frac{-(r-c_6)^2}{2\sigma_6^2}}\right) \\ & \times \mathrm{Max}\left(e^{\frac{-(\theta_1-c_7)^2}{2\sigma_7^2}}, e^{\frac{-(\theta_1-c_8)^2}{2\sigma_8^2}}\right) \\ = {} & 1, \quad c_1 < c_2,\ c_3 < c_4,\ c_5 < c_6,\ c_7 < c_8 \end{aligned} \tag{4}$$

where $(c_1,\sigma_1,c_2,\sigma_2)=(0, 10, 500, 500)$, $(c_3,\sigma_3,c_4,\sigma_4)=(0, 10, 30, 10)$, $(c_5,\sigma_5,c_6,\sigma_6)=(0, 10, 500, 500)$, and $(c_7,\sigma_7,c_8,\sigma_8)=(210,10, 360, 10)$ are examined to be valid. The values of $c_i$ $(i=1,8)$ denotes the mean that identifies the storm range at rank 7 in the Area 1 or Area 4. The values of $\sigma_i(i=1,8)$ indicating the variance determine the shape of the functional curve. The parameters $c_i$ and $\sigma_1$ are commonly called by the location and shape parameter of the normal distribution, respectively. When the Hua-Lien harbor is beyond the range of a 500-km circle of a typhoon, $MF_1=1$. When the Hua-Lien harbor is located within this range, the waves at the Hua-Lien harbor increases as the radial distance decreases. When the typhoon is near the Hua-Lien harbor, the wind speeds vary fast. When the typhoon is far from the Hua-Lien harbor, the wind speeds change slowly. Thus the variances $\sigma_1=\sigma_5=10$ km are accepted, and $\sigma_2$ and $\sigma_6$ are assumed to be 500 km. All variations on $\theta_1$ during the typhoon movement are assumed to be 10°. The south–north line for separating areas is inclined by an angle of about 30°. Thus, the mean angle $\theta_1$ of each port is set by 0°, 30°, 210° and 360°.

Most of the typhoons that pass through or by the eastern Taiwan start around the western Pacific Ocean and move westwards. However, some typhoons form around the China South Sea and pass through Taiwan. These typhoons of which the positions are still at the western Taiwan have little effect on the waves of the Hua-Lien harbor at the eastern coast of Taiwan. The second component of the membership function, $MF_2$ shown in Eq. (5), clarifies rapidly decaying of waves when a typhoon is approaching from Area 1 to Area 2. For the case, the Hua-Lien harbor is always situated at the left semicircle of the typhoon.

$$\begin{aligned} MF_3(r,\theta_1) = {} & \mathrm{Max}\left(e^{\frac{-(r-c_1)^2}{2\sigma_1^2}}, e^{\frac{-(r-c_2)^2}{2\sigma_2^2}}\right) \\ & \times \mathrm{Max}\left(e^{\frac{-(\theta_1-c_3)^2}{2\sigma_3^2}}, e^{\frac{-(\theta_1-c_4)^2}{2\sigma_4^2}}\right) \\ = {} & 1, \quad c_1 < c_2, \quad c_3 < c_4 \end{aligned} \tag{5}$$

where $(c_1,\sigma_1,c_2,\sigma_2)=(0,10, 30, 10)$ and $(c_3,\sigma_3,c_4,\sigma_4)=(180, 10, 210, 10)$. When $r\approx 30$ km, the high mountains in the central Taiwan have strong effects on wave decaying. Thus $c_1=0$ and $c_2=30$ km are accepted, and the variances, $\sigma_1$ and $\sigma_2$, of $r$ are reasonably set as 10 km. The variances, $\sigma_3$ and $\sigma_4$, of $\theta_1$ are still assumed to be 10° for the case. The mean angle $\theta_1$ for $c_3$ and $c_4$ is 180° and 210°.

The third component, $MF_3$ illustrates wind decaying of a typhoon approaching from Area 4 to Area 3. For this case, the Hua-Lien harbor is always situated at the right semicircle of the typhoon. Thus $MF_3$ can be also expressed by Eq. (5) but with different $(c_1,\sigma_1,c_2,\sigma_2)=(0, 10, 70, 10)$ and $(c_3,\sigma_3,c_4,\sigma_4)=(30, 10, 80, 10)$ are examined to be valid. The valid $MF_2$ and $MF_3$ represent different wind decaying after examinations. The membership function shown in Fig. 6 will be finally determined by maximizing these three possible components as follows

$$MF(r,\theta_1) = \mathrm{Max}\{MF_1,\ MF_2,\ MF_3,\ 0.2\} \tag{6}$$

Eq. (6) shows that the minimum of $MF(r,\theta_1)$ is set 0.2 rather than 0. The required minimum confirms the output larger than 0.

### 3.2. The algorithm of fuzzy–neural hybrid model

Following 24-h time lag well examined in the NN–MT model, the positions of a typhoon during 24 h form a proceeding distance vector, $\mathbf{r}(t)=[r(t-24),\ r(t-23),\ \ldots,\ r(t)]$, and a proceeding azimuth vector, $\boldsymbol{\theta}_1(t)=[\theta_1(t-24),\ \theta_1(t-23),\ \ldots,\ \theta_1(t)]$ at time $t$. Both vectors have 25 elements which indicate the distance and azimuth, respectively, between the center of the typhoon and the point of interest at each hour. A rule of fuzzy inference system is given as

$$\begin{aligned} &\text{If} \quad r=(t) \wedge \theta_1=\theta_1(t) \quad \text{is} \quad M(t) \quad \text{and} \\ &r=r(t-1) \wedge \theta_1=\theta_1(t-1) \quad \text{is} \quad M(t-1),\ldots, \quad \text{and} \\ &r=r(t-24) \wedge \theta_1=\theta_1(t-24) \quad \text{is} \quad M(t-24) \quad \text{then} \\ &H_s(t)=f(\mathbf{W}\cdot\mathbf{I}_{FN}(t)+\mathbf{b}) \end{aligned} \tag{7}$$

where $\mathbf{I}_{FN}(t)=[M(t)H_{sMT}(t),\ M(t-1)H_{sMT}(t-1),\ \ldots,\ M(t-24)H_{sMT}(t-24)]$ is the input vector also including 25 elements that are the product of the membership function and the wave height obtained by the NN–MT model and $M(t-i)=MF(r,\theta_1;\ t-i)$ which is the linguistic label of fuzzy sets denoting the membership functions when a typhoon moves to $(r,\theta_1)$ at time $t-i$ $(i=1,2,\ldots,n)$, respectively.

The membership function depending on the degree of a typhoon approaching to the Taiwan shows the correction on local winds and waves due to land effect. The membership

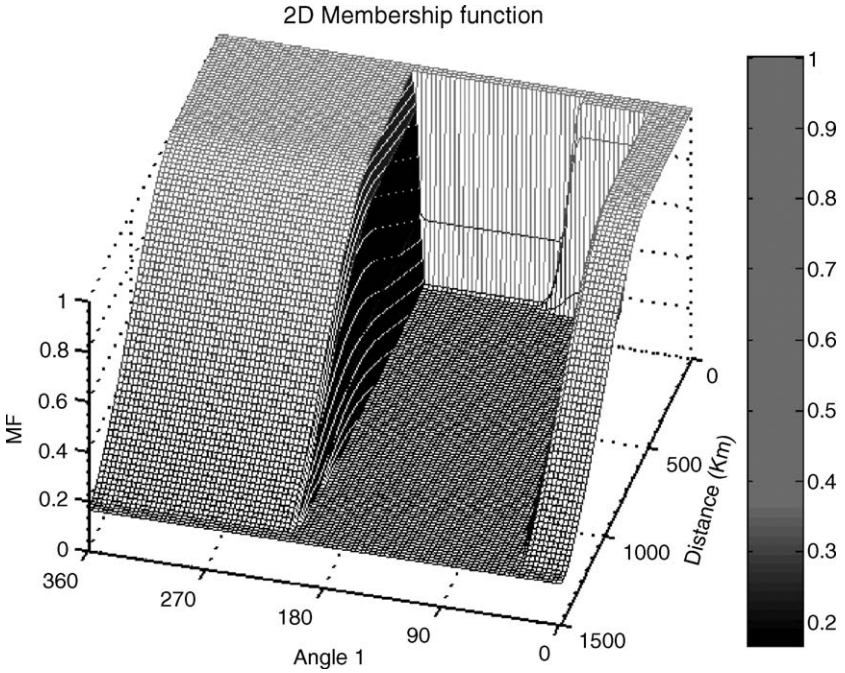


Fig. 6. The proposed membership function MF($r$,$\theta_1$).

function is expressed in terms of two variables, $r$ and $\theta_1$. The wind speed $V_{10}$, and the angles of $\theta_1$, and $\theta_2$ of the point of interest together depends on $r$ and rapidly vary due to land effect. The fast variations of $V_{10}$, $\theta_1$, and $\theta_2$ when a typhoon is near the Taiwan differ from those when a typhoon is far from away Taiwan. Therefore, the membership function is used to correct the original values $V_{10}$, $\theta_1$, and $\theta_2$ in the NN–MT model.

Eq. (7) represents corrected typhoon waves resulting from possible paths of typhoons. All possible paths of typhoons are various so that the weights are determined by a second neural network. This hybrid system incorporates the original NN–MT model and a corrected NN model associated with membership functions of fuzzy technologies. The proposed NN model including fuzzy technologies is thus called by the fuzzy–neural hybrid wave model, abbreviated as (FN). The proposed FN wave model is similar to adaptive-network-based fuzzy inference system. ANFIS uses a hybrid learning algorithm to identify the membership function parameters of single-output, Sugeno-type fuzzy inference systems. A combination of least-squares and back-propagation gradient descent methods is used for training FIS membership function parameters to model a given set of input/output data. Therefore, the parameters in a chosen membership function of ANFIS usually depend on obtained data. If the number of valid data too less to train the membership function, the parameters in the membership function obtained may be unreasonable. Another difficulty is that the complexity of land effect on wind distribution and waves is described by lots of IF–THEN rules in FIS so that it takes much computational time in the training process. To overcome the disadvantages, the proposed membership functions are specified to have suitable location and shape parameters for each quarter portion considering the in-site land topography. These parameters are used only for the Hua-Lien harbor and are not changed by different training data. However, the corrected simulation on waves due to the land effect is made by another NN model with the optimal weight and bias matrices which are obtained in the training process.

### 3.3. The construction of the proposed FN wave model

The first possible network is to correct the input vectors in the NN–MT model by multiplying the membership function mentioned above. The other network is to multiply the outputs of the NN–MT model, the pre-calculated wave heights, by the membership of function. Based on the aspects of two possible modifications on the wave heights predicted, two wave models are proposed in this paper.

The NF1 model includes three stages. The construction of the FN1 model is depicted in Fig. 7. The first stage of the FN1 model is the same as that of the NN–MT model to normalize the four inputs and have the basic input vector $I_{\mathrm{MT}}$. In the second stage multiplying the membership function MF($r$,$\theta_1$) yields the corrected input vector, that is $I_{\mathrm{FN1}}(t)=I_{\mathrm{MT}}\times\mathrm{MF}(r,\theta_1)$. The third

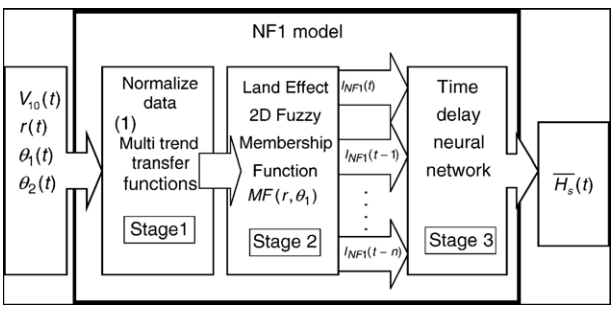


Fig. 7. The construction of the proposed FN1 model.

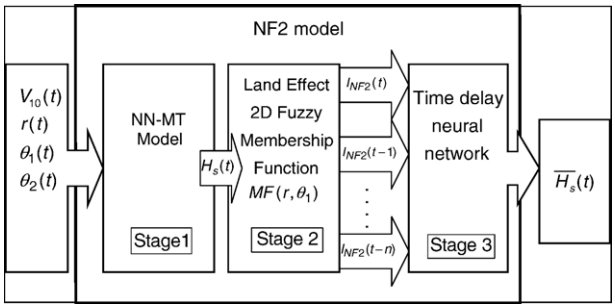


Fig. 8. The construction of the proposed FN2 model.

stage is to provide the BPN network with the corrected input vector in a sequence of 24 h which is connected to the wave heights. The mathematical expression for the FN1 model is similar to Eq. (3) in which $I_{FN1}$ is instead of $I_{MT}$.

The FN2 model of which the construction is shown in Fig. 8 also comprises three stages. In the first stage the NN–MT model is used to obtain pre-calculated wave heights in which the land effect is excluded. The membership function MF($r$,$\theta_1$) is first computed in the second stage and then multiplied by the pre-calculated wave heights to have the corrected input vector $I_{FN2}(t)=[H_{sMT}(t)]\times MF(r,\theta_1)$. The BPN network is used in the third stage to have optimal weight and bias matrices showing the sequential 24-h wind effect on waves. The input vector in this BPN network is $I_{FN2}(t-n)$.

In the third stage of both models, BPN network with two hidden layers is used to obtain optimal weight matrix and bias matrix by minimizing the error square of the outputs computed and the normalized wave heights measured. A 24-h time lag is also considered in the proposed model. To aid the computation time, each input is simultaneously selected from time series for every 4 h instead of every hour, i.e., at the time $t$, $t-4$, $t-8$,..., $t-24$. Thus, the total number of inputs equals seven variables in the input vector times seven time steps and is 49. The neurons in the first hidden layer are 80, and 40 neurons in the second hidden layer. The proposed FN1 model is thus designated by (49–80–40–1). The inputs of the second BPN network of the FN2 models in a sequence at the time $t$, $t-4$, $t-8$, ..., $t-24$. The total number of inputs is 7. The neurons in the first hidden layer are 60, and 20 neurons in the second hidden layer. The FN2 model is thus designated by (7–60–20–1).

## 4. Model calibration

Typically, an applicable BPNN model is validated in both the learning stage and the verification stage. When the errors of each iteration in both the learning stage and the verification stage are simultaneously decreasing, the model continues to learn. Conversely, whenever the error magnifies, the model stops learning. When the simulation error reaches the assigned minimum, the optimal weight and the bias matrices have been set. To simulate typhoon waves accurately, the model must pass the verification stage. The iteration stops in the learning stage when the maximum iteration is over 5000 times or the root mean square (RMS) of the target function of each iteration is less than 0.1 m.

The data of typhoon's position and scale were obtained from the Central Weather Bureau of Taiwan (CWB; http://www.cwb.gov.tw/), the Joint Typhoon Warning Center (JTWC; http://manati.wwb.noaa.gov/) and UNISYS WEATHER (http://weather.unisys.com/). The name of the typhoon given by JTWC and Greenwich Mean Time (GMT) were used. The typhoon data were sampled every 6 h. Third-order Lagrangian interpolation for transforming 6 h of typhoon data into 1 h of data was applied to match the 1-h wave data. Fig. 9 plots the path of nine typhoons examined in the learning stage.

Commonly the simulation performance of a model is evaluated by the root mean square (RMS) and correlation coefficients ($R$). The root mean square is defined as

$$\mathrm{RMS}=\sqrt{\frac{1}{m}\sum_{i=1}^{m}\left[H_{sm}(t_i)-H_{sp}(t_i)\right]^2} \tag{8}$$

where $H_{sm}(t_i)$ and $H_{sp}(t_i)$ represent the observed and calculated wave height at time $t_i$, respectively, and $m$ is the total number of data. The correlation coefficient identifies the degree of correlation between $H_{sm}(t_i)$ and $H_{sp}(t_i)$. The maximum wave height and its occurrence time are very important in practical engineering. Two alternative indices of simulation performance are given by the difference between the peak observed wave height and the corresponding calculated value, $\Delta H_{sp}$, and time lag between the corresponding times, $\Delta t_p$, as follows

$$\Delta H_{sp}=H_{sp,p}-H_{sp,m} \tag{9}$$

$$\Delta t_p=t_{p,p}-t_{p,m} \tag{10}$$

where $H_{sp,m}$ and $H_{sp,p}$ are the observed and calculated peak wave heights, respectively; $t_{p,m}$ and $t_{p,p}$ are the times at which these peaks occur.

Four performance indices for the simulated waves by the NN–MT, FN1 and FN2 models in the learning stage are list in Table 2. The values of $R$ in Table 2 indicate that the FN2 model has the values of $R$ higher than 0.6 for seven cases, and the NN–MT model obtains the values of $R$ of six cases higher than 0.6, but the values of $R$ of only one case obtained by the FN1 model is less than 0.6. This shows that the FN1 model can better simulate the behaviors of wave growth and wave decaying of each typhoon similar to those observed than do the NN–MT and FN2 models. From the comparison on $R$ in Table 2, the NN–MT and FN2 models have equivalent capacity of simulating the wave growth and wave decaying.

Comparisons on RMS and RMS/$H_{sp,m}$ in Table 2 show that the FN2 model is the best model among the three models to have small RMS less than 0.73 m or relative RMS/$H_{sp,m}$ less than 19%. In common cases examined by the FN2 model, the values of RMS less than 0.4 m or relative RMS/$H_{sp,m}$ less than 15% indicates that the FN2 model can be applicable for accurately calculating the typhoon wave heights. Averaging the RMS of nine typhoons yields 0.52, 0.78 and 0.48, respectively. The FN1 model estimates commonly larger RMS and RMS/$H_{sp,m}$ than do the NN–MT and FN2 models.

From comparisons of $\Delta H_{sp}$ and $\Delta H_{sp}/H_{sp,m}$, the FN1 model is the worst one of calculating the peak wave height

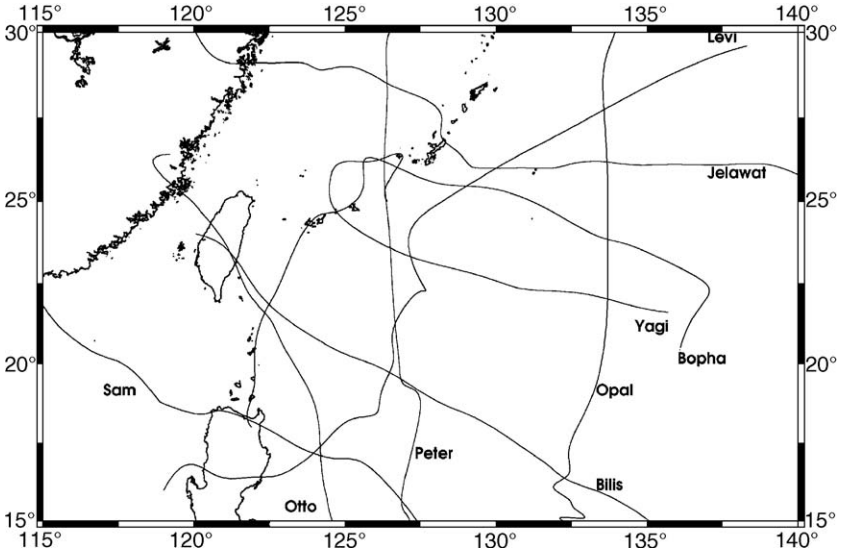


Fig. 9. Paths of nine typhoons considered in the learning stage.

among three models. The NN–MT model has good estimate on the peak wave height by an error less than 1.0 m or by a relative error less than 25%. In most cases the relative error of $\Delta H_{sp}/H_{sp,m}$ obtained by the NN–MT model is less than 12%. The FN2 model can also precisely calculate by an error of $\Delta H_{sp}$ less than 1.2 m. There are seven cases examined by the FN2 model to have a relative error of $\Delta H_{sp}/H_{sp,m}$ greater than 15%. This shows that the FN1 model is a slightly worse predictor on the peak of wave heights than the NN–MT and FN2 models.

These three models compared have equivalent capacity of determining the occurrence time of the peak wave heights of each typhoon. The largest difference between the estimated and the observed occurrence time is 5 h. The FN1 and FN2 models can precisely estimate the occurrence time of the peak wave height by less than 3 h for six cases.

After the comparisons on the simulation accuracy, the FN1 model generally has worse simulation performance than do both the NN–MT and FN2 models. The direct correction on the input vector in the FN1 model adds the complexity of simulation to the BPN network. The FN1 model using the same learning data as the NN–MT model becomes tricky to simulate the wave heights. The disadvantage can be overcome by increasing the number of valid data. However, the FN2 model using the membership function to directly and efficiently modify the wave heights pre-calculated is capable of simulating wave heights affected by the land.

## 5. Model verification

After model calibration of the proposed models is well done, the model verification will be then examined to identify the

Table 2
Comparisons of $R$, RMS, $\Delta H_{sp}$ and $\Delta t_p$ obtained using the NN–MT, FN1, and FN2 models in the learning stage

| Model and typhoon | | Levi | Opal | Peter | Otto | Sam | Jelawat | Bilis | Boph | Yagi |
|---|---|---|---|---|---|---|---|---|---|---|
| $R$ | NN–MT | 0.47 | 0.36 | 0.88 | 0.91 | 0.91 | 0.31 | 0.86 | 0.88 | 0.66 |
| | NF1 | 0.66 | 0.66 | 0.84 | 0.77 | 0.84 | 0.26 | 0.78 | 0.89 | 0.80 |
| | NF2 | 0.50 | 0.39 | 0.90 | 0.88 | 0.90 | 0.63 | 0.90 | 0.88 | 0.67 |
| RMS (m) | NN–MT | 0.52 | 0.25 | 0.32 | 0.89 | 0.44 | 0.51 | 0.65 | 0.45 | 0.63 |
| | NF1 | 0.57 | 0.39 | 0.40 | 0.94 | 0.65 | 0.80 | 1.03 | 1.22 | 1.02 |
| | NF2 | 0.31 | 0.37 | 0.30 | 0.68 | 0.54 | 0.28 | 0.70 | 0.39 | 0.73 |
| $\frac{RMS}{H_{sp,m}}$ | NN–MT | 0.27 | 0.13 | 0.10 | 0.11 | 0.11 | 0.27 | 0.08 | 0.16 | 0.22 |
| | NF1 | 0.30 | 0.20 | 0.13 | 0.12 | 0.17 | 0.42 | 0.12 | 0.44 | 0.35 |
| | NF2 | 0.16 | 0.19 | 0.12 | 0.08 | 0.14 | 0.15 | 0.08 | 0.14 | 0.25 |
| $\Delta H_{sp}$ (m) | NN–MT | 0.37 | 0.02 | −0.36 | −1.00 | 0.37 | −0.10 | −0.52 | 0.22 | 0.24 |
| | NF1 | 0.74 | −1.00 | −0.17 | −1.62 | −0.91 | 0.90 | −2.14 | 2.50 | 1.20 |
| | NF2 | 0.06 | −0.20 | −0.48 | −0.96 | −0.34 | −0.02 | −1.20 | 0.30 | 1.00 |
| $\frac{\Delta H_{sp}}{H_{sp,m}}$ | NN–MT | 0.19 | 0.01 | 0.11 | 0.12 | 0.10 | 0.05 | 0.06 | 0.08 | 0.08 |
| | NF1 | 0.25 | 0.51 | 0.05 | 0.20 | 0.24 | 0.47 | 0.26 | 0.90 | 0.42 |
| | NF2 | 0.03 | 0.10 | 0.15 | 0.12 | 0.09 | 0.01 | 0.14 | 0.11 | 0.35 |
| $\Delta t_p$ (h) | NN–MT | 5 | 0 | 0 | 0 | 2 | −2 | −3 | 5 | 4 |
| | NF1 | 5 | 0 | 0 | 0 | −4 | −2 | −5 | −2 | 4 |
| | NF2 | 5 | 0 | 0 | 0 | 2 | 0 | −3 | 5 | 4 |
| $H_{sp,m}$ | | 1.92 | 1.97 | 3.19 | 8.03 | 3.89 | 1.97 | 8.39 | 2.78 | 2.89 |

Table 3
Comparisons of $R$, RMS, $\Delta H_{sp}$ and $\Delta t_p$ obtained using the NN–MT, NF1, and NF2 in the verification stage

| Model and typhoon | | Fred | Kent | Haiyan | Rananim | Aere | Maggie[a] |
|---|---|---|---|---|---|---|---|
| $R$ | NN–MT | 0.90 | 0.87 | 0.83 | 0.71 | 0.53 | 0.93 |
| | NF1 | 0.90 | 0.82 | 0.84 | 0.85 | 0.88 | 0.95 |
| | NF2 | 0.94 | 0.92 | 0.82 | 0.89 | 0.89 | 0.87 |
| RMS (m) | NN–MT | 0.53 | 0.59 | 0.47 | 0.70 | 1.63 | 0.72 |
| | NF1 | 0.35 | 0.79 | 0.51 | 0.56 | 0.73 | 0.53 |
| | NF2 | 0.35 | 0.45 | 0.51 | 0.39 | 0.68 | 0.66 |
| $\frac{RMS}{H_{sp,m}}$ | NN–MT | 0.08 | 0.10 | 0.10 | 0.21 | 0.24 | 0.12 |
| | NF1 | 0.05 | 0.13 | 0.11 | 0.17 | 0.18 | 0.09 |
| | NF2 | 0.05 | 0.07 | 0.11 | 0.12 | 0.17 | 0.11 |
| $\Delta H_{sp}$ (m) | NN–MT | 0.45 | −1.14 | −0.30 | 0.51 | 1.42 | −0.11 |
| | NF1 | 0.10 | −0.50 | −0.10 | 0.44 | 0.61 | −2.00 |
| | NF2 | 0.50 | −1.14 | −0.30 | 0.51 | 0.60 | 0.30 |
| $\frac{\Delta H_{sp}}{H_{sp,m}}$ | NN–MT | 0.07 | 0.18 | 0.02 | 0.16 | 0.35 | 0.02 |
| | NF1 | 0.01 | 0.08 | 0.07 | 0.13 | 0.15 | 0.34 |
| | NF2 | 0.07 | 0.18 | 0.07 | 0.16 | 0.15 | 0.05 |
| $\Delta t_p$ (h) | NN–MT | 1 | −1 | 0 | 0 | 23 | 1 |
| | NF1 | −1 | 2 | 0 | −2 | 10 | 0 |
| | NF2 | 1 | 0 | 0 | 0 | 5 | 0 |
| $H_{sp,m}$ (m) | | 6.75 | 6.29 | 4.49 | 3.29 | 4.09 | 5.96 |

[a] The simulation for the Su-Ao harbor.

capacity of accurately calculating typhoon's waves in this section. Comparisons on the results simulated by the three developed models for six typhoons that are excluded in the training data are list in Table 3. Five typhoons are chosen for simulating wave heights at the Hua-Lien harbor. They are typhoons Fred in 1994, Kent in 1995, Haiyan in 2001, Rananim, and Aere in 2004. The proposed models are also applied to calculating the wave heights at the Su-Ao harbor during the period of typhoon Maggie in 1999. Except the typhoon Haiyan five typhoons are affected by the Taiwan. The paths of six typhoons are depicted in Fig. 10.

A comparison on $R$ in Table 3 shows that, except for two $R$ values obtained by the NN–MT model for typhoon Rananim and typhoon Aere, most of the $R$ values are higher than 0.8 and that the FN2 model has higher $R$ than do the other two models for four typhoons. Comparisons on RMS indicate that the proposed FN1 and FN2 models have slightly larger RMS for typhoon Haiyan than does the NN–MT model by only 0.04 m, but for the other five typhoons the proposed FN1 and FN2 models have significantly smaller RMS than does the NN–MT model. These results show that the proposed FN1 and FN2 models have better calculation on typhoon waves for the whole period of a typhoon than does the NN–MT model. The mean RMS of the wave heights simulated by the NN–MT, FN1 and FN2 models are 0.77, 0.58, and 0.51, respectively. For most cases, the FN2 model having the smallest RMS among three the models identifies the best simulation capability.

From a comparison on the peak wave heights, although the FN1 model is very poor to simulate the peak of typhoon Maggie, both the NN–MT and FN2 models provide rather good simulations. The range of absolute value of $\Delta H_{sp}$ obtained by the FN1 and FN2 models is 0.10–2.00 m, and 0.50–1.14 m. Their corresponding mean values are 0.66 and 0.56, respectively. The occurrence time of the peak wave simulated is shown in the last row group of Table 3. The FN2 models demonstrate accurate simulation on the occurrence time of the peak. Except of the typhoon Area, the FN2 model can have exact simulation of the occurrence for four typhoons, and only 1-h delay prediction for typhoon Fred.

The capacity of simulating typhoon's wave heights affected by the land using the proposed FN1 and FN2 can be illustrated for three typhoons in time series. After typhoon Fred was formed and then traveled for 300 h, it passed through the north of the island. Fig. 11 plots the wave heights computed by the NN–MT, FN1 and FN2 models. The time counts from the formation of the typhoon. When typhoon Fred arrived in Taiwan, the Hua-Lien harbor was under the left half of the typhoon. The peak wave heights computed by the NN–MT model for the period in which wind waves grew exceeded the observed heights by around 0.45 m. The NN–MT model simulated 1-h time delay after the actual peak. When typhoon

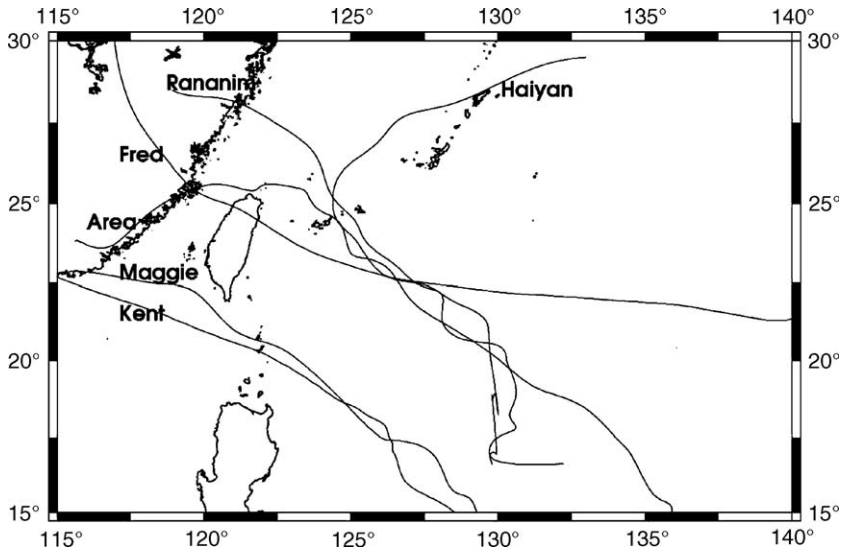


Fig. 10. Paths of six typhoons used in the verification stage.

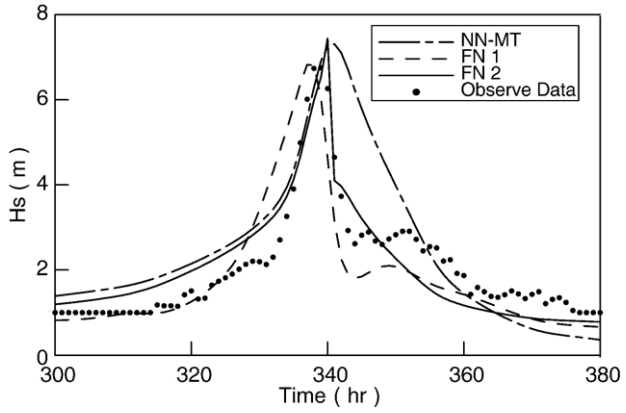


Fig. 11. Wave heights observed and computed at the Hua-Lien harbor for typhoon Fred in 1994.

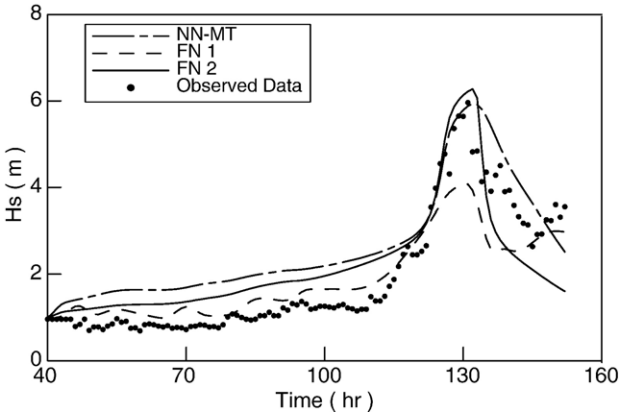


Fig. 13. Wave heights observed and computed at the Hua-Lien harbor for typhoon Maggie in 1999.

Fred passed Taiwan, observed wave heights decayed very fast due to very high mountains in central Taiwan and the computed wave heights decayed slowly because of higher wind speeds input in the model than the real values. The land effect on winds whenever a typhoon passes through Taiwan can not be well predicted. Both the FN1 and FN2 models can provide quite good calculation on the decaying waves when the typhoon Fred approaches Taiwan.

Fig. 10 shows that typhoon Rananim moved westwards to Taiwan and then turned northwest, and finally reached the eastern China. Fig. 12 plots the computed and observed wave heights for the typhoon Rananim. As the waves grew, the wave heights computed by the NN–MT and FN2 models fairly agree with the observed heights. The peaks simulated by both NN–MT and FN2 models are close and have a deviation from the observed peak by about 0.51 m. Both models exactly simulate the occurrence time of the peak wave height. However, the FN1 model has 2-h delay prediction on the occurrence time of the peak wave height. The FN1 and FN2 models have better simulations on the decaying waves than does the NN–MT model.

Only one wave record of typhoon Maggie at the Su-Ao harbor was available for extending the proposed models to the Su-Ao harbor. Typhoon Maggie originally formed over the waters to the southeast of Taiwan and moved northwestward, passing through the Bashi Channel, finally reaching southeast China. Fig. 13 shows the simulated and observed wave heights during typhoon Maggie. While typhoon Maggie was far from the Su-Ao harbor, the computed wind speeds exceed the real wind speeds because the Su-Ao harbor was then located in the right semicircle of typhoon Maggie. The simulated wave heights by the FN2 model approximately exceed by 0.3 m from the observed heights. The NN–MT and FN2 models simulate the wave heights much better than does the FN1 model when typhoon Maggie approximately arrived in Taiwan. When the typhoon Maggie passes through the Bashi Channel, the land effect happens and the waves rapidly decay. The FN2 model can accurately response to the decaying waves. Through the examination on the wave heights predicted for the typhoon Maggie at the Su-Ao harbor, the proposed FN2 model is proven to be applicable for calculating the typhoon waves at a point of interest along the Taiwan eastern coast.

From detailed comparison on the waves simulated in time series, the land effect on the waves can be validly simulated by the FN2 models.

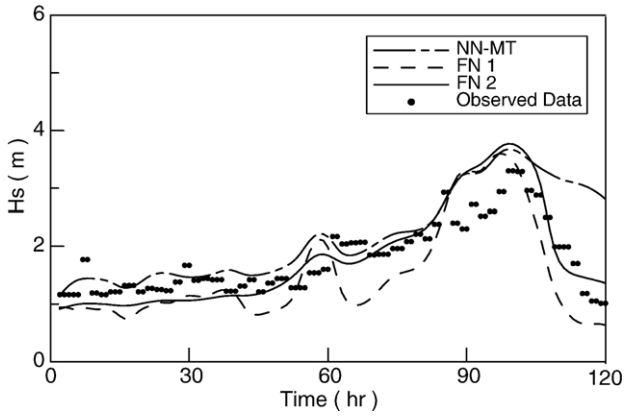


Fig. 12. Wave heights observed and computed at the Hua-Lien harbor for typhoon Rananim in 2004.

## 6. Conclusions

The marine structures in Taiwan have been suffered from typhoon attacks in the summer time every year. Sometimes people and properties are lost during the period of typhoon approaching. Therefore, a marine alarm system that needs to provide fast information of wave conditions and storm surge at some important coastal sites when predicted path and scale of the typhoon are given will be established. The authors have developed some neural network wave models to meet the requirement of rapidly simulating typhoon waves. However, the high mountains in Taiwan play important role in altering the wind speed and distribution of a typhoon. Thus the previous models without considering the land effect have poor simulation on the wave decaying when a typhoon is near Taiwan and is affected by the land.

The authors considered the land effect on waves to propose two kinds of fuzzy–neural hybrid systems of simulating typhoon waves. The fuzzy theory is applied to setup a membership function of land effect on waves. This membership function in terms of two independent parameters that are the radial distance and the azimuth is expressed by a union Gaussian function in which the location and shape parameters are specified considering the performance of real data plot. When a typhoon is near the point of interest, the membership function plays a sharp decrease by the Gaussian function for describing the wave decaying. The valid mean and variance in the Gaussian function are examined for four areas separated by two lines which intersect at the Hua-Lien harbor.

The FN1 model that directly corrects the original input vector used in the previous NN–MT model by multiplying the membership function and then connects to the wave heights by a back-propagation neural network needs more learning data for the expected complexity of wave varying by the land than does the previous NN–MT model. When new data are available to be added in the learning data set or the membership function is modified, the weight and bias matrices in the FN1 model has to be determined by relearning the whole latest data. It is disadvantageous for the FN1 model to take long time for renewing the weight and bias matrices when wind and wave data used in the learning stage are different or the membership function is modified.

The FN2 model includes two back-propagation neural networks. The first network is the previous one in the NN–MT model, and the second network considers a time sequence of input vector and two hidden layers. The membership function is used to correct the output wave heights that are calculated by the first network as a corrected input vector for the second network. The FN2 model needs more learning time than the FN1 due to an extra network. Because the previous NN–MT model has good simulation on the peak wave height and its occurrence time, the FN2 model directly corrects on the pre-estimated wave heights by multiplying the membership function so that the FN2 model has good simulation on wave decaying.

The better simulation performances of the peak wave heights and their occurrence time in both the learning stage and the verification stage by the FN2 model and the previous NN–MT models than by the FN1 model identify the high capacity of simulated typhoon waves. The FN2 model has slightly better simulation on the occurrence time of the peak of typhoon waves by an error of less than 3 h in common cases than does the NN–MT model. The wave decaying due to land effect is well described by the FN2 model. The FN2 model is examined to have good simulation on the peak, occurrence time and wave decaying of typhoon waves even when the typhoon arrives in Taiwan. Most typhoons used in both the learning stage and the verification stage move westwards from the Pacific Ocean. Thus a typhoon with a particular path, i.e. south-to-north or eastward movement, cannot be well simulated by the proposed models. The disadvantage can be improved by adding the data of which the typhoon path is south-to-north, or eastward into the original learning data and renewing the weight and bias matrices.

## References


Agrawal, J.D., Deo, M.C., 2002. On-line wave prediction. Mar. Struct. 15, 57–74.

Balas, C.E., Levent, K., Balas, L., 2004. Predictions of missing wave data by recurrent neuronets. J. Waterw. Port Coast. Ocean Eng. 130, 256–265.

Bardossy, A., Duckstein, L., Bogardi, I., 1995. Fuzzy rule-based classification of atmospheric circulation patterns. Int. J. Climatol. 15, 1087–1097.

Bishop, C.T., Donelan, M.A., Kahma, K.K., 1992. Shore protection manual's wave prediction reviewed. Coast. Eng. 17, 25–48.

Bretschneider, C.L., Tamaye, E.E., 1976. Hurricane wind and wave forecasting techniques. Proc. of the 15th Conf. on Coastal Eng., Hawaii, vol. 1, pp. 202–237.

Chang, H.K., Chien, W.A., 2006. Neural network with multi-trend simulating transfer function for forecasting typhoon wave. Adv. Eng. Softw. 37, 184–194.

Chang, H.K., Chien, W.A., Ho, L.S., 2003. Neural network models of typhoon waves in the waters east of Taiwan. J. Ocean Coast. Eng. 3, 73–95 (in Chinese).

Demuth, H., Beale, M., 2001. Neural network toolbox for use with MATLAB, user's guide. Natick, MA: The MathWorks Inc.

Deo, M.C., Jagdale, S.S., 2003. Prediction of breaking waves with neural networks. Ocean Eng. 30, 1163–1178.

Deo, M.C., Kiran Kumar, N., 2000. Interpolation of wave heights. Ocean Eng. 27, 907–919.

Deo, M.C., Shidhar Naidu, C., 1998. Real time wave forecasting using neural networks. Ocean Eng. 26, 191–203.

Deo, M.C., Jha, A., Chaphekar, A.S., Ravikant, K., 2001. Neural networks for wave forecasting. Ocean Eng. 28, 889–898.

Deo, M.C., Gondane, D.S., Sanil Kumar, V., 2002. Analysis of wave directional spreading using neural networks. J. Waterw. Port Coast. Ocean Eng. 128, 30–37.

Donelan, M.A., 1980. Similarity theory applied to the sea forecasting of wave heights, periods and directions. Proc. Canadian Coastal Conf., pp. 47–61.

Donelan, M.A., Hamilton, J., Hui, W.H., 1985. Directional spectra of wind-generated waves. Phil. Trans. R. Soc., A 315, 509–562.

Dubrovin, T., Jolma, A., Turunen, E., 2002. Fuzzy model for real-time reservoir operation. J. Water Resour. Plan. Manage. 128 (1), 66–73.

Galambosi, A., Duckstein, L., Özelkan, E., Bogardi, I., 1998. A fuzzy rule-based model to link circulation patterns, ENSO and extreme precipitation. In: Haimes, Y.Y., Moser, D., Stakhiv, E.Z. (Eds.), Risk-Based Decision Making in Water Resources: VIII. ASCE Press, New York, pp. 83–102.

Goda, Y., 2003. Random Seas and Design of Marine Structures. World Scientific, Singapore. 443 pp.

Hasselmann, K.K., Barnett, T.P., Bouws, E., Carlson, H., Cartwright, D.E., Enke, E., Ewing, J.A., Gienapp, H., Hasslelmann, D.E., Kruseman, P., Meerburg, A., Muller, P., Olbers, D.J., Richter, K., Sell, W., Walden, H., 1973. Measurements of wind-wave growth and swell decay during the Joint North Sea Wave Project (JONSWAP). Dtsch. Hydrogr. Z., Suppl. A 8 (12), 95.

Hiraoka, T., Maeda, H., Ikoma, N., 1999. Two-stage prediction method of typhoon position by fuzzy modeling-fusion of outline prediction and detailed prediction systems. Proc of IEEE SMC '99 Conf on Man, and Cybernetics, vol. 6, pp. 581–585.

Hsu, T.W., Ou, S.H., Liau, J.M., 2005. Hindcasting nearshore wind waves using a FEM code for SWAN. Coast. Eng. 52, 177–195.

Hurdle, D.P., Stive, M.J.F., 1989. Revision of SPM 1984 wave hindcast model to avoid inconsistencies in engineering applications. Coast. Eng. 12, 339–357.

Koylov, Y.M., 1966. Spectral Methods of Studying and Predicting of Wind Waves. Gidrometeoizdat, Leningrad. 256 pp.

Lippman, R.P., 1987. An introduction to computing with neural nets. IEEE ASSP Mag. 4, 14–24.

Makarynskyy, O., 2004. Improving wave predictions with artificial neural networks. Ocean Eng. 31, 709–724.

Massel, S.R., 1996. Ocean Surface Waves: their Physics and Prediction. World Scientific, Singapore. 491 pp.

Mirchandani, G., Cao, W., 1989. On hidden nodes for neural nets. IEEE Trans. Circuits Syst. 36 (5), 661–664.

Ponnambalam, K., Karray, F., Mousavi, S.J., 2003. Optimization of reservoir systems operation using soft computing tools. Fuzzy Sets Syst. 139 (2), 451–461.

Russel, S.O., Camplell, P.E., 1996. Reservoir operating rules with fuzzy programming. J. Water Resour. Plan. Manage. 122 (3), 165–170.

Shore Protection Manual, 1984. U.S. Army Coastal Engineering Research Center, Fort Belvoir, Vol. I–III.

Shrestha, B.P., Duckstein, L.E., Stokhin, Z., 1996. Fuzzy rule-based modeling of reservoir operation. J. Water Resour. Plan. Manage. 122 (4), 262–269.

Yu, P.S., Chen, S.-T., Chen, C.-J., Yang, T.-C., 2005. The potential of fuzzy multi-objective model for rainfall forecasting from typhoons. Nat. Hazards 34 (2), 131–150.